Available online at www.sciencedirect.com

ScienceDirect

Procedia Technology 25 (2016) 107 – 114

Procedia Technology

Global Colloquium in Recent Advancement and Effectual Researches in Engineering, Science and Technology (RAEREST 2016)

# Early-age Temperature Distribution in a Massive Concrete Foundation

Bennet Kuriakose[a,b,*], B. Nageswara Rao[a], G. R. Dodagoudar[a]

[a]*Indian Institute of Technology Madras, Chennai 600 036, India*
[b]*Mangalam College of Engineering, Ettumanoor 686 631, India*

**Abstract**

Early-age cracking appertains to massive concrete elements on the account of thermal gradients due to highly exothermic hydration reaction of cement. The cracking as a result of thermal strains can in turn lead to undesirable consequences on structural durability. In this paper, a degree of hydration-based finite element simulation procedure is developed and implemented in order to determine the temperature distribution of young concrete within a massive solid circular raft foundation. The developed finite element program is validated with experimental results available in the literature. The information regarding temperature development can effectively be used to compute thermal stresses while designing the massive foundation for structural as well as durability considerations. Appropriate measures can also be taken to bring down the temperature levels during the phased casting operations so as to avoid early-age cracking problems.

Peer-review under responsibility of the organizing committee of RAEREST 2016

*Keywords:* Early-age cracking; mass concrete; degree of hydration; numerical model; phased casting.

## 1. Introduction

The early age behaviour of concrete has proven to be decisive with regard to massive concrete constructions like thick foundations, roller compacted dams, piers, etc. Hardening of fresh concrete associated with exothermic chemical hydration process, raises the temperature of the concrete within the domain of the structure. The cooling of the massive concrete results in considerable thermal gradients primarily attributed to the low thermal conductivity of the young concrete. These thermal gradients aggregated with external as well as internal restraint to volume changes

* Corresponding author. Tel.: +91-481-2710120.
*E-mail address:* bennet.kuriakose@mangalam.in


Peer-review under responsibility of the organizing committee of RAEREST 2016
doi:10.1016/j.protcy.2016.08.087

induce stresses. These stresses if surpass the limits, induce cracking, especially 'through cracking', which covers the full thickness of the massive concrete [1]. As a result of this, potential self-induced damage can occur in the structure well before the action of working loads.

In view of the imperceptible influence of the mechanical field of concrete on the thermal evolution and hydration process, it is customary to consider a unidirectional coupling in which, the stress analysis is performed after the thermal computations [2]. The temperature distribution in concrete structures and its evolution with time depends on thermal parameters such as evolving concrete properties, ambient conditions, placement temperature, phased casting operation sequence, etc., making the problem highly non-linear [3]. Many researchers have proposed different approaches for numerical simulation of temperature distribution in early age concrete [1-5]. A degree of hydration - based finite element formulation [6] for the simulation of the thermal profile of thick reinforced concrete circular raft foundation during its early age is presented in this paper. The computed temperature data can be utilised for mechanical analysis of concrete raft so as to evaluate the resulting thermal stresses and hence the possible risk of cracking.

**Nomenclature**

| | |
|---|---|
| $\chi$ | number of moles of water combined with cement |
| $\xi$ | degree of hydration |
| $\dot{Q}$ | rate of heat production |
| $f(\xi)$ | normalised chemical affinity function |
| $k$ | conductivity |
| $C$ | volumetric specific heat capacity |
| $T$ | temperature |
| $h_c$ | convection coefficient |
| $t$ | time |

## 2. Modelling of Concrete Hydration

The prominent mechanism associated with the chemical kinetics of hydrating cement is observed to be dispersion of water. The number of moles of water combined with cement at any instant $\chi$ can be utilised to charecterise the chemical demeanour of concrete. A normalised format is often preferred for convenience, so that the term 'degree of hydration' is defined as[7]

$$\xi = \frac{\chi}{\overline{\chi}_\infty} \tag{1}$$

where, $\overline{\chi}_\infty$ being the ideal value of $\chi$ at infinite time. In practical situations, the full hydration of cement will never be attained and the ultimate hydration degree $\xi_\infty$ is always less than unity [8]. The rate of heat production due to the hydration of concrete, $\dot{Q}$ can be expressed in terms of $f(\xi)$, called as normalised chemical affinity and $g(T)$, which is the function describing the influence of temperature on heat production as [9]

$$\dot{Q} = Q_\xi \cdot f(\xi) \cdot g(T) \tag{2}$$

where, $Q_\xi$ is the maximum value of the heat produced at 20°C isothermal hydration. It is customary to denote Eq. (2) in terms of rate of hydration as $\dot{Q} = Q_\xi \dot{\xi}$, and the rate of degree of hydration $\dot{\xi}$ can be expressed using an Arrhenius function in the following form [10]:

$$\dot{\xi} = f(\xi)\exp\left(-\frac{E_a}{R\,T}\right) \geq 0 \tag{3}$$

where, $E_a$ is the activation energy (Jmol$^{-1}$), $R$ is the universal gas constant (8.314 J mol$^{-1}$K$^{-1}$). Normally, the normalised affinity of hydrating concrete is derived from the adiabatic curve of the concrete [9] or alternatively, in absence of experimental data, is determined according to the empirical expression [11]:

$$f(\xi) = \frac{m}{n_0}\left(\frac{A_0}{m\xi_\infty} + \xi\right)(\xi_\infty - \xi)\exp\left(-\frac{\bar{n}\,\xi}{\xi_\infty}\right) \tag{4}$$

where, $A_0$ is the initial affinity of the reaction (when $\xi = 0$) whereas, $m$, $n_0$ and $\bar{n}$ are material constants depending on the type of cement.

## 3. Governing Differential Equation

According to the principles of thermodynamics, a system undergoing thermal changes is assumed to be governed by the field equation [12]

$$\dot{H} + \dot{D} - \nabla\Phi_{\mathrm{f}} + \dot{Q} = C\dot{T} \tag{5}$$

where, $\dot{H}$ denotes the rate of external heat generation, $\dot{D}$ denotes the dissipation, $\Phi_{\mathrm{f}}$ is the heat flux and $C$ denotes the volumetric specific heat capacity. For ordinary concrete, the volumetric specific heat typically ranges between 2.04 and 2.76 kJ/m$^3$K [5]. Concerning the problem of hydration of concrete, the external heat source and the dissipation can be neglected [7]. Employing the Fourier's law ( $\Phi_{\mathrm{f}} = -k\,\nabla T$ ), the thermal field equation takes the form:

$$k\,\nabla \cdot \nabla T + \dot{Q} = C\dot{T} \tag{6}$$

Thermal conductivity, $k_\infty$ for ordinary hardened concrete ranges between 1.2 and 3.5 W/mK and the conductivity of early age concrete evolves according to [8]

$$k = k_\infty(1.33 - 0.33\,\xi) \tag{7}$$

## 4. Boundary Conditions

If the temperature at a boundary is known, it can be considered as a Dirichlet boundary condition, where the temperature, $\bar{T}$ is prescribed along the boundary. The other heat transfer ways can be expressed via heat flux along the normal to the boundary $\Gamma_q$, popularly known as Newmann boundary condition [13]. Convection is a term that refers to the heat transfer occurring between the concrete surface and a moving fluid. The convective heat transfer can be expressed using Newton's cooling law as [8]

$$q = h_c\,(T_S - T_{env}) \tag{8}$$

where, $q$ is the convective heat flux per unit area, $h_c$ is the convection coefficient, $T_s$ is the surface temperature and $T_{env}$ is the ambient temperature of the surrounding air. In the absence of accurate data, the diurnal variation of the air temperature can be assumed to follow a sinusoidal cycle between the maximum and minimum values. Daily ambient maximum and minimum temperatures ($T_{\max}$ and $T_{\min}$) can be used to predict the ambient temperature at any time, with the following variation [4]:

$$T_{env} = -\sin\left(\frac{2\pi(t_d + t_m)}{24}\right)\left(\frac{T_{\max} - T_{\min}}{2}\right) + \left(\frac{T_{\max} + T_{\min}}{2}\right) \tag{9}$$

where, $t_d$ is the clock time of day at which the prediction is being made (0 to 24 hours) and $t_m$ is the time at which the minimum overnight temperature occurs (usually just at sunrise).

## 5. Finite Element Implementation

The standard procedure of the finite element method (FEM) is followed, whereby, temperature $T$ is expanded over an element by $T = \boldsymbol{N}\boldsymbol{T^e}$, where, $\boldsymbol{N}$ denotes the matrix of shape functions and $\boldsymbol{T^e}$ designates the nodal temperatures for a given element with volume $\Omega$ . Now, the weak form of the field equation accounting for the boundary conditions becomes [6]:

$$\int_{\Omega} \boldsymbol{N}^T C \dot{T}\, \mathrm{d}\Omega + \int_{\Omega} \nabla \boldsymbol{N}^T k \nabla T\, \mathrm{d}\Omega = \int_{\Omega} \boldsymbol{N}^T \dot{Q}\, \mathrm{d}\Omega - \int_{\Gamma_q} \boldsymbol{N}^T q\, \mathrm{d}\Gamma_q \tag{10}$$

This equation is written in terms of time $t_{n+1}$ and assuming unconditionally stable backward-Euler time integration scheme of the form

$$\dot{T}_{n+1} = \frac{(T_{n+1} - T_n)}{\Delta t} \tag{11}$$

with $\Delta t$ being the time-step between two consecutive instants $t_n$ and $t_{n+1}$, leads one to the following set of algebraic equations, which is suitable for implementation in a computer program:

$$\frac{1}{\Delta t}\boldsymbol{C}^e\left(\boldsymbol{T}^e_{n+1} - \boldsymbol{T}^e_n\right) + \boldsymbol{H}^e\,\boldsymbol{T}^e_{n+1} = \boldsymbol{F}^e_T + \boldsymbol{F}^e_Q \tag{12}$$

where, the elemental matrices and vectors in this equation are computed according to [7]

$$\begin{aligned}
\boldsymbol{C}^e &= \int_{\Omega} \boldsymbol{N}^T C \boldsymbol{N}\, \mathrm{d}\Omega \\
\boldsymbol{H}^e &= \int_{\Omega} \nabla \boldsymbol{N}^T k \nabla \boldsymbol{N}\, \mathrm{d}\Omega + \int_{\Gamma_q} \boldsymbol{N}^T h \boldsymbol{N}\, \mathrm{d}\Gamma_q \\
\boldsymbol{F}_T{}^e &= \int_{\Gamma_q} \boldsymbol{N}^T h_{eq} T_A\, \mathrm{d}\Gamma_q \\
\boldsymbol{F}_Q{}^e &= \int_{\Omega} \boldsymbol{N}^T \dot{Q}_{n+1}\, \mathrm{d}\Omega
\end{aligned} \tag{13}$$

The standard assembly procedure may be followed to compose the global matrices and vectors so as to arrive at the following equation:

$$\left(\frac{\boldsymbol{C}}{\Delta t}+\boldsymbol{K}\right)\boldsymbol{T}_{n+1}=\boldsymbol{F}_{T}+\boldsymbol{F}_{Q}+\frac{\boldsymbol{C}}{\Delta t}\boldsymbol{T}_{n} \tag{14}$$

The interdependency of the hydration rate and temperature necessitates the following two level iterative procedures to be implemented in the highly non-linear finite element procedure to solve Eqn. (14): (i) at the global level (i.e., in the matrices and vectors), due to the nonlinear dependency of $\boldsymbol{F}_Q$ on $\boldsymbol{T}_{n+1}$ and (ii) at the local level (i.e., at each integration point), due to the nonlinear dependency of $\xi$ on the $T$. The detailed discussion on the algorithm for the rigorous numerical procedure for heat transport problem for early-age concrete is available in Kuriakose et al. [7].

## 6. Results and Discussion

In order to demonstrate the abovementioned finite element procedure, computer programs in MATLAB environment have been developed and implemented using the following numerical examples. The results of the present study have highlighted the necessity and practical applicability of the proposed methodology in engineering practice.

### *6.1. Validation Example*

The proposed methodology is applied to a problem given by Faria et al. [9] in order to determine the temperature distribution in the concrete at early ages. The problem concerns a reinforced concrete floor slab with very tight constraints for the differential vertical deflections under the service loads. The slab is 143 m long, 41 m wide and 0.35 m thick, supported on piles arranged in a 3 × 4 $m^2$ mesh. A simplification results in a one-dimensional (1D) non-linear heat transfer problem along the thickness of the slab. The thermal properties of concrete and the other relevant data are available in the literature [9]. Considering the unit width, the slab is discretised into seven 8-noded planar elements along the thickness. The conductivity ($k$) along horizontal direction is input as zero in order to accomplish a compatible 1D transport.  The temperature evolution at a point 50 mm from the top of the slab is presented in Fig. 1. These results are compared with those reported in the literature [9] and found to be in good agreement.

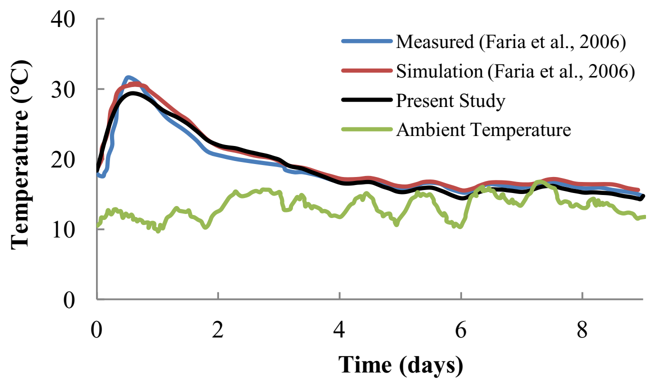


Fig. 1. Temperature history at a point 50 mm from top of the 0.35 m thick slab.

### 6.2. Case Study: Thick Circular Raft

After validating the finite element formulation, a case study involving a circular raft of 12 m diameter and 3 m thick, founded on a solid granite bedrock is considered (Fig. 2). The raft forms foundation for a 100 m high ventilation stack associated with a fast breeder type nuclear reactor. The raft is constructed via two phased casting operations, i.e., 1.5 m thick concrete is poured at once and remaining thickness is cast after 3 days.

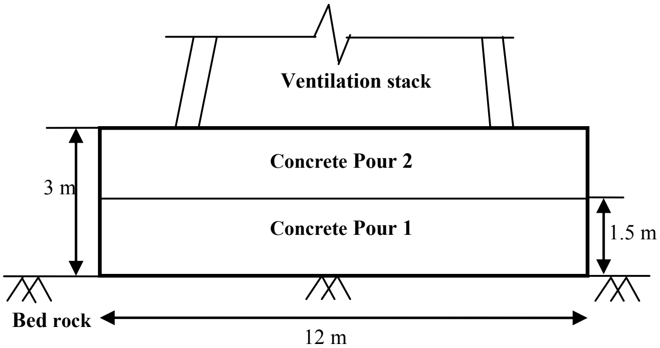


Fig. 2. Geometry of the circular raft.

The thermal conductivity of concrete $(k_c)$ of the foundation is considered to be evolving as 2.6 × (1.33- 0.33 $\xi$ ) W/mK, whereas the conductivity of bedrock $(k_r)$ is considered to be 2.8 W/mK [3]. The values of volumetric specific heat of both concrete $(C_c)$ and rock $(C_r)$ adopted for the current problem are 2400 kJ/m$^3$K [9] and 2040 kJ/m$^3$K [3], respectively. The Eqns. (2) - (4) for the present study are formulated using the following parameters: $Q_\infty = 2.5\times 10^8$ J/m$^3$, $\xi_\infty = 0.96$, $A_0 / k = 1\times10^{-5}$, $\overline{n} = 6$, $k / n_0 = 0.35 \times 10^8$ h$^{-1}$ and $E_a / R = 5000$ K [5]. The initial temperature of rock massif is considered as 25°C whereas the placement temperature of both the pours of the concrete is taken as 19°C. The environmental temperature is accounted based on $T_{env} = 10\sin\left(\frac{\pi t_{days}}{12}\right) + 25$ °C. Taking advantage of the axial symmetry, the two-dimensional (2D) domain is discretised using 8-noded planar elements as shown in Fig. 3. Two types of boundary are considered, viz., boundary 1 (free contact with air) with convection coefficient value of 10 W/m$^2$K and boundary 2 (wood shuttering) with a value of 7.5 W/m$^2$K. The phased casting of raft foundation is simulated employing the birth of element technique [15].

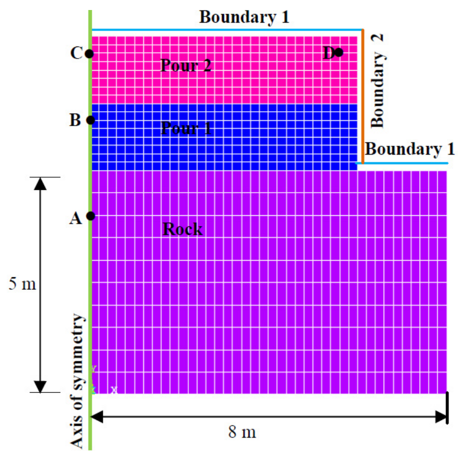


Fig. 3. Finite element discretisation of the circular raft.

The temperature evolutions at 3 points (A, B, C) along the axis of the raft and at another point D (refer Fig. 3), which are located at different heights of the domain from the instant of the first pour till 7 days are depicted in Fig. 4. The temperature profile of the raft at 2 days and 5 days of age is portrayed in Fig. 5. It can be noted from the Figs. 4 and 5 that, once the first pour is cast, the temperature of the pour increases and gradually decreases in the course of time especially due to the convective heat transfer at the boundaries. When the second pouring is performed, heat generated during the hydration further increases the temperature of the concrete in pour 1 as well as a part of the granite massif. Furthermore, it can be noted that hydration of cement raises the temperature at the core of each of the concrete pours, producing considerable differential temperatures with respect to the outer portion of the concrete (approximately 20°C), which induces a risk of through cracking. Fig. 6 depicts the evolution of degree of hydration ($\xi$) at three points (B, C and D) of the raft. This information can be further input into a mechanical analysis scheme so as to arrive at the stresses and crack widths.

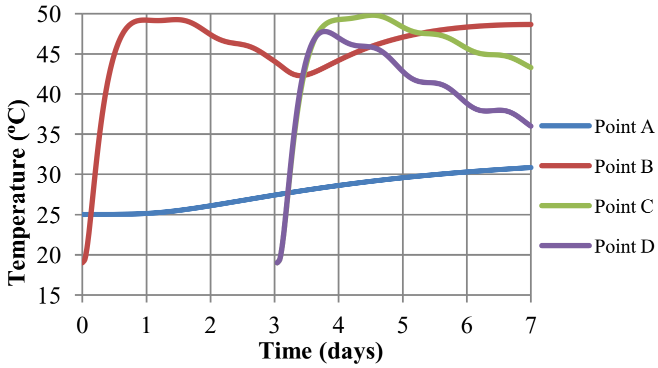


Fig. 4. Temperature evolutions at four different points in the circular raft.

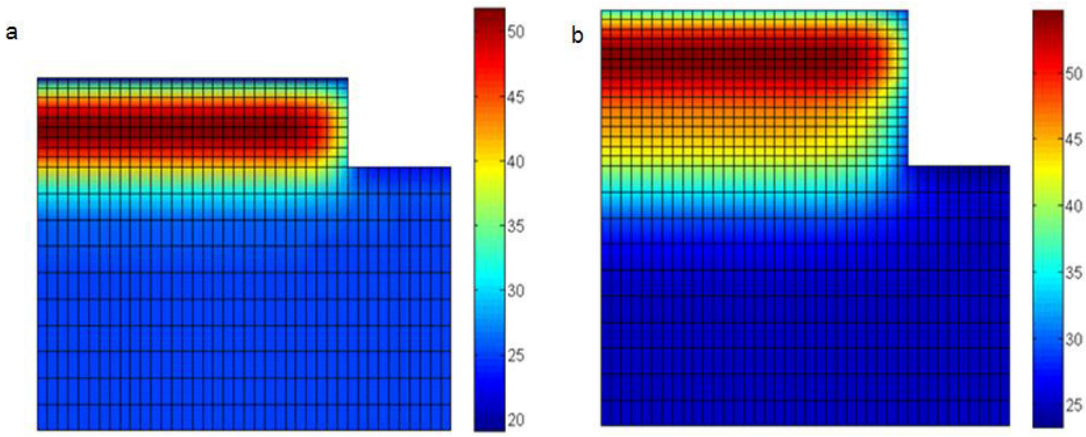


Fig. 5. Temperature (°C) profile of the raft at (a) 2 days and (b) 5 days.

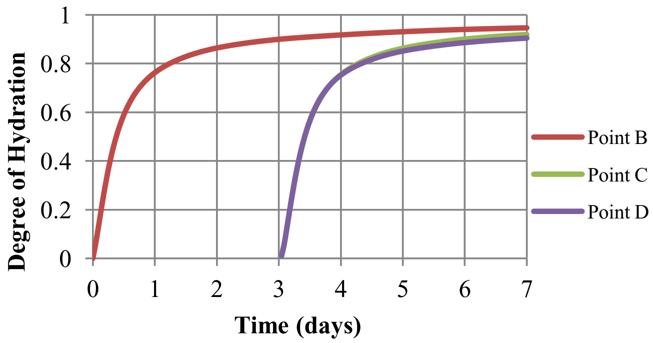


Fig. 6. Hydration process at three different points of the raft

## 7. Conclusions

The finite element simulation technique is used to numerically compute the evolution of temperature due to hydration of concrete during the construction phase of the thick circular raft foundation. A two dimensional formulation based on the degree of hydration theory is used for the formulation of the finite element procedure. The developed finite element program has been validated with the experimental results. For the raft of 3 m thickness and consisting of distinct pours cast in two-phased casting sequence, a large variation in temperature is noted and is sustained for longer duration during the construction. This information can be used appropriately while designing the raft for structural serviceability considerations. This also helps one to adopt appropriate measures to bring down the temperature levels of the raft, so as to avoid cracking during and immediately after the casting operations.

## References

[1] Amin MN, Kim J-S, Lee Y, Kim J-K. Simulation of the thermal stress in mass concrete using a thermal stress device. Cement Concrete Res 2009; 39:154-164.
[2] de Borst R, van den Boogaard AH. Finite-element modeling of deformation and cracking in early-age concrete. J Eng Mech-ASCE 1994; 120(12):2519-2534.
[3] Azenha M, Faria R, Ferreira D. Identification of early-age concrete temperatures and strains: monitoring and numerical simulation. Cement Concrete Comp 2009; 31(6):369-378.
[4] Ballim Y. A numerical model and associated calorimeter for predicting temperature profiles in mass concrete. Cement Concrete Comp 2004; 26(6):695-703.
[5] van Breugel K. Prediction of temperature development in hardening concrete. In: Springenschmid R, editor. Prevention of thermal cracking in concrete at early ages. London: E&FN Spon; 1998.
[6] De Schutter G. Hydration and temperature development of concrete made with blast-furnace slag cement. Cement Concrete Res 1999; 29(1):143-149.
[7] Kuriakose B, Rao BN, Dodagoudar GR, Venkatachalapathy V. Modelling of heat of hydration for thick concrete constructions – a note. J Struct Eng- Madras 2015; 42(4):348-357.
[8] Cervera M, Faria R, Oliver J, Prato T. Numerical modelling of concrete curing, regarding hydration and temperature phenomena. Comput Struct 2002; 80(18-19):1511-1521.
[9] Faria R, Azenha M, Figueiras JA. Modelling of concrete at early ages: Application to an externally restrained slab. Cement Concrete Comp 2006; 28(6):572-585.
[10] De Schutter G. Finite element simulation of thermal cracking in massive hardening concrete elements using degree of hydration based material laws. Comput Struct 2002; 80(27-30):2035-2042.
[11] Azenha M, Lameiras R, de Sousa C, Barros J. Application of air cooled pipes for reduction of early age cracking risk in a massive RC wall. Eng Struct 2014; 62-63:148-163.
[12] Cervera M, Oliver J, Prato T. Simulation of construction of RCC dams. I: Temperature and aging. J Struct Eng-ASCE 2000; 126(9):1053-1061.
[13] Cervera M, Oliver J, Prato T. Thermo-chemo-mechanical model for concrete. I: Hydration and aging. J Eng Mech-ASCE 1999; 125(9):1018-1027.
[14] Holman JP. Heat Transfer. New York:McGraw-Hill; 1997.
[15] Cook RD, Malkus DS, Plesha ME, Witt RJ. Concepts and application of finite element analysis. Singapore: John Wiley and Sons (Asia) Pte. Ltd.; 2005.